Electromagnetic scattering from a buried three-dimensional inhomogeneity in a lossy ground

Kristensson, Gerhard

Published in:
Technical Report

1979

79-29

August, 1979

Electromagnetic scattering from a buried three-dimensional inhomogeneity in a lossy ground[†]

by

Gerhard Kristensson

[†]This work was supported by the National Swedish Board for Technical Development (STU).

Institute of Theoretical Physics

S-412 96 GÖTEBORG

Sweden

Abstract

The T matrix method (also called the "extended boundary condition method" or "null field approach") introduced by Waterman, has recently been generalized to interfaces of infinite extent (G. Kristensson and S. Ström, J. Acoust. Soc. Am. 64, 917-936 (1978) and G. Kristensson, "Electromagnetic Scattering from Buried Inhomogeneities - a General Threedimensional Formalism", Rep. 78-42, Inst. of Theoretical Physics, Göteborg (1978), to appear in J. Appl. Phys.). This paper extends the formalism to lossy materials. Here we explicitly assume that the ground and the inhomogeneity have losses, but the formalism also applies to a lossy medium above the ground with only minor changes. In developing the theory, we assume the source to be situated above the ground but it is otherwise arbitrary. A similar formalism can be constructed when the source position is located in the ground or in the inhomogeneity. The scattered field is calculated both above and below the ground. Above the ground the scattered field separates into two parts, which have direct physical interpretation; one field, here called the directly scattered field, which is the total scattered field when no buried obstacle is present, and a second field, the anomalous field, which reflects the presence of the inhomogeneity. We present some numerical computations of the field both above and below the ground for a flat earth and a buried perfectly conduction spheroid. The main theoretical developments are given in an appendix, where we study the transformation between plane and spherical vector waves for a complex wave number.

I Introduction

Waterman [1] originally developed the T matrix method of scattering from a scatterer of finite extent (cf. also [2] for the elastic case). This approach (also called the "extended boundary condition method" or "null field approach") has been generalized to scattering from a buried inhomogeneity in the lossless case for both acoustic, electromagnetic and elastic waves [3] - [5]. The present paper will extend the formalism to the lossy case, which in many scattering problems is the situation of greatest interest. The scattering configuration will be truly three dimensional, and the formalism contains rather weak assumptions on the source distributions, the geometry of the scatterer etc. We will here explicitly develop the scattering formalism for electromagnetic waves with a source above the ground but the results are applicable with appropriate modifications to the acoustic and elastic cases and sources in other regions of interest.

The integral representation of the field is the basic element in the formalism. Suitable expansions of the Green's dyadic are central in the method and depending on the situation it is expanded in either plane or spherical vector waves. The transformation properties between these two elementary waves - plane and spherical - play an important part in the formalism and we analyse its properties in the lossy case in detail. The plane and spherical waves also enter in the expansions of the pertinent surface fields.

The inhomogeneity is completely described by its T matrix referring to spherical waves. The T matrix enters in the formalism as a building block in the construction of the solution, and in

this context many results derived from scattering from obstacles of finite extent can be used. The interaction between the ground and the inhomogeneity is described by the solution of a matrix equation, where a power series expansion of the inverse of the matrix formally can be identified as multiple scattering contributions [3], [4]. We will in this paper study this matrix equation for the lossy case, and give explicit expressions in the flat interface case. Both the field above and below the ground are analysed and explicit expressions are given in the flat earth case.

The electromagnetic scattering from a source, say a dipole, in the presence of a homogeneous halfspace has been studied thoroughly and a long list of references are given in [4] addressing themselves to this problem, both with and without an inhomogeneity present in one of the halfspaces. Many of these treatments are purely numerical, while others pursue an analytic solution of the problem.

In section II the scattering problems to be considered are defined, the fundamental assumptions are introduced and the basic equations derived, while in section III the use of the formalism is illustrated in some numerical examples. In an appendix, we analyse the transformation properties between plane and spherical waves in the lossy case for both scalar and vector waves as needed for the theory developed in section II.

II T matric formalism for a lossy ground

Basic equations

In this section we will point out the essential differences and similarities between the lossless case [4], and the situation where losses are present in the ground and the inhomogeneity. Most equations are identical in structure to the corresponding lossless ones, and at some instances we will therefore be rather brief and we refer to [4] for more details.

Consider a scattering geometry as depicted in Fig. 1. The surface S_o separates the halfspaces V_o and V_1, which are assumed to be homogeneous except for a finite region V_2. This inhomogeneity is bounded by the surface S_1. Besides the implicit assumptions on the surfaces S_o and S_1, namely that they fulfil the necessary regularity conditions for an application of the Green's theorem, we also assume S_o to lie between the two parallel planes $z=z_>$ and $z=z_<$ (the z-axis is defined as perpendicular to these planes). We assume that the source and the inhomogeneity are located in separate halfspaces (the source location is marked with a P). A parallel formulation can be made when both source and inhomogeneity occupy the same halfspace [3] or the source is inside the obstacle. Furthermore we will in this context permit the different regions to have losses. In many practical applications one encounters a situation where the halfspace V_o can be assumed to be lossless, and this is the explicit case we will consider here. The introduction of losses also in V_o is straightforward and the details are left to the reader.

In each volume the electric field $\vec{E}_i$ satisfies (we assume

the time factor $e^{-i\omega t}$ throughout this paper)

$$\nabla \times \nabla \times \vec{E}_i(\vec{r}) - k_i^2 \vec{E}_i(\vec{r}) = \vec{0} \qquad \vec{r} \text{ in } V_i \; ; \; i = 0,1,2 \tag{1}$$

Here $k_i^2 = \omega^2 \mu_o \varepsilon_o \varepsilon_{i_r} \mu_{i_r} + i\omega\sigma_i \mu_{i_r} \mu_o$ $i=0,1,2$, where ε_o and μ_o are the dielectric constant and permeability of free space and σ_i the conductivity in V_1. As discussed above we will in this paper only consider the case $\sigma_o = 0$. All equations in this paper will explicitly be written down for the electric field $\vec{E}_i$. The same analysis holds for the $\vec{H}_i$ field, and what is discussed below about the $\vec{E}_i$ field can equally well be applied to the magnetic field $\vec{H}_i$ if we interpret the source distributions as the corresponding magnetic ones, e.g. an electric dipole becomes a magnetic dipole, and the necessary substitutions are made, see Eq. (2) below.

The boundary conditions are continuity in the tangential magnetic and electric fields on the surface S_o and S_1 (for notations see Fig. 1), i.e.

$$\begin{cases} \hat{n}_i \times \vec{E}_i^+(\vec{r}') = \hat{n}_i \times \vec{E}_{i+1}^-(\vec{r}') \\ \hat{n}_i \times [\nabla' \times \vec{E}_i^+(\vec{r}')] = c_i \, \hat{n}_i \times [\nabla' \times \vec{E}_{i+1}^-(\vec{r}')] \\ c_i = \mu_{i_r} / \mu_{i+1_r} \qquad i = 0,1 \end{cases} \qquad \vec{r}' \in S_i \; ; \; i = 0,1 \tag{2}$$

(If we replace $\vec{E}$ with $\vec{H}$, let $c_i = \left(\frac{k_i}{k_{i+1}}\right)^2 \mu_{i+1_r} \mu_{i_r}^{-1}$.)

The starting point in the T matrix formalism [1] is the following integral representation of the field $\vec{E}$ in terms of a surface integral over the tangential components of $\vec{E}$ and $\vec{H}$ on the bounding surface S.

$$\left.\begin{matrix}\vec{E}(\vec{r}) \\ \vec{0}\end{matrix}\right\} = \vec{E}^{inc.}(\vec{r}) + \nabla \times \iint_S \hat{n} \times \vec{E}^{+}(\vec{r}') \, G(\vec{r},\vec{r}';k) \, dS' +$$

$$+ k^{-2} \nabla \times \left\{ \nabla \times \iint_S \hat{n} \times (\nabla' \times \vec{E}^{+}(\vec{r}')) \, G(\vec{r},\vec{r}';k) \, dS' \right\} \qquad (3)$$

$$\begin{cases} \vec{r} \text{ outside } S \\ \vec{r} \text{ inside } S \end{cases}$$

S is a bounded surface and $\vec{E}^{+}$ and $\nabla \times \vec{E}^{+}$ are the field values on the outside of S ($\hat{n}$ is directed outwards on S). The Green's function $G(\vec{r},\vec{r}';k)$ satisfies the Helmholtz' equation with a delta function source term.

$$(\nabla^2 + k^2) \, G(\vec{r},\vec{r}';k) = -\delta(\vec{r}-\vec{r}') \qquad (4)$$

The requirement of an outgoing wave at infinity gives us the solution to Eq. (4)

$$G(\vec{r},\vec{r}';k) = \exp(ik|\vec{r}-\vec{r}'|) \,/\, 4\pi|\vec{r}-\vec{r}'| \qquad (5)$$

It should be noted here that k can be a complex number, which will be the case when we apply Eq. (3) to volumes with losses.

As discussed in [4] both plane and spherical vector waves are introduced as well as the transformation between these. In these quantities we must justify the analytic continuation of k-values into the complex plane. The definition of spherical waves are found in [4]. The extension to complex k values in these definitions introduces no problems; the complex quantities just appear in the

radial dependence argument kr but leave the spherical vector harmonics $\vec{A}_n(\hat{r})$ unaffected. The transformation between spherical and plane vector waves are discussed in detail in the appendix and we have, (see Eq. (A.22)):

$$\vec{\Psi}_n(k\vec{r}) = \frac{i}{2\pi}\int_0^{2\pi} d\beta \int_{C_\pm} \vec{B}_n(\hat{k})\, e^{i\vec{k}\cdot\vec{r}} \sin\alpha\, d\alpha \qquad z \gtrless 0 \tag{6}$$

The complex contours $C_\pm$ are depicted in Fig. 2 (see the appendix for a definition of the contours). The contour C_+ - the upgoing waves - is used when $z>0$ and C_- - the downgoing waves - when $z<0$. It should be noted that along the $C_\pm$ contours $k\sin\alpha$ is real and that Eq. (6) essentially is a two-dimensional Fourier integral in k_x, k_y rewritten in the spherical angles (α,β) of $\vec{k}$, i.e. $\vec{k}=k(\sin\alpha\cos\beta,\ \sin\alpha\sin\beta,\ \cos\alpha)$. The definition of $\vec{B}_n(\vec{k})$ is found in [4]:

$$\vec{B}_{\tau n}(\hat{k}) = i^{\tau-2-l}\,\vec{A}_{\tau n}(\hat{k}) \qquad \tau = 1,2 \tag{7}$$

Note that we here, and when convenient also below, abbreviate the indices as follows $n\equiv\tau n\equiv\tau\sigma ml$. As a special case ($l=0$) of Eq. (A.15) we also get the plane wave expansion of the Green's function in Eq. (5)

$$G(\vec{r},\vec{r}';k) = \frac{ik}{8\pi^2}\int_0^{2\pi} d\beta \int_{C_\pm} e^{i\vec{k}\cdot(\vec{r}-\vec{r}')} \sin\alpha\, d\alpha \qquad z \gtrless z'$$

The Green's dyadic $\overleftrightarrow{I}G(\vec{r},\vec{r}';k)$ can thus be written [4]:

$$\overleftrightarrow{I}G(\vec{r},\vec{r}';k) = \sum_{j=1}^{3} \frac{ik}{8\pi^2}\int_0^{2\pi} d\beta \int_{C_\pm} \hat{a}_j\hat{a}_j\, e^{i\vec{k}\cdot(\vec{r}-\vec{r}')} \sin\alpha\, d\alpha \qquad z \gtrless z' \tag{8}$$

Here $\overleftrightarrow{I}$ is the unit dyadic and $\hat{a}_j$, j=1,3 are the spherical unit vectors of $\hat{k}=\vec{k}/k$ and with the following convention:

$$\hat{a}_1 = \hat{\alpha}$$
$$\hat{a}_2 = \hat{\beta}$$
$$\hat{a}_3 = \hat{k}$$

The separation of the Green's dyadic in spherical vector waves is found in e.g. [6]:

$$\overleftrightarrow{I}G(\vec{r},\vec{r}';k) = ik\sum_{\substack{n \\ \tau=1,2}} \mathrm{Re}\vec{\psi}_n(k\vec{r}_<)\,\vec{\psi}_n(k\vec{r}_>) + \overleftrightarrow{I}_{irr.} \qquad (9)$$

The argument $\vec{r}_>$ and $\vec{r}_<$ are chosen to be $\vec{r}$ or $\vec{r}'$ according to $|\vec{r}_<| = \min(r,r')$, $|\vec{r}_>| = \max(r,r')$ and the dyadic $\overleftrightarrow{I}_{irr.}$ is an irrotational dyadic. Eq. (9) holds for complex values of k, at least for values of k in our domain of interest, i.e. $\arg k \in [0,\pi/4)$ [7]. In analogy with Eq. (6) we also need the transformation between the regular spherical vector waves and the plane waves. This is found in e.g. [8]:

$$\mathrm{Re}\vec{\psi}_n(k\vec{r}) = \frac{i}{4\pi}\int_0^{2\pi} d\beta \int_0^{\pi} \vec{B}_n(\hat{k})\, e^{i\vec{k}\cdot\vec{r}} \sin\alpha\, d\alpha \qquad (10)$$

The extension to complex values of k in this integral over a finite interval causes no problems and the formula holds in the common domain of analyticity of the two sides.

We now apply the integral representation Eq. (3) to a surface S consisting of a finite part of S_o and lower half sphere. Assume that the fields encountered in the integral over the lower half-sphere satisfy the appropriate radiation condition. As the

radius of the half sphere approaches infinity this integral then vanishes. By introducing the plane wave expansion of the Green's dyadic, see Eq. (8), in the surface integral over S_o we obtain the following plane wave expansions of the scattered and incoming field, respectively (which are formally the same as in the lossless case):

$$\vec{E}_o^{sc.}(\vec{r}) = \int_0^{2\pi} d\beta_o \int_{C_+} \vec{f}(\vec{k}_o)\, e^{i\vec{k}_o\cdot\vec{r}} \sin\alpha_o\, d\alpha_o \qquad z > z_> \tag{11}$$

$$\vec{E}_o^{inc.}(\vec{r}) = \int_0^{2\pi} d\beta_o \int_{C_-} \vec{a}(\vec{k}_o)\, e^{i\vec{k}_o\cdot\vec{r}} \sin\alpha_o\, d\alpha_o \qquad z < z_< \tag{12}$$

$$f_j(\vec{k}_o) \equiv \frac{ik_o}{8\pi^2} \iint_{S_o} \left\{ (\hat{n}_o \times \vec{E}_o^+)\cdot(\hat{a}_j \times i\vec{k}_o) + [\hat{n}_o \times (\nabla' \times \vec{E}_o^+)]\cdot\hat{a}_j \right\} e^{-i\vec{k}_o\cdot\vec{r}'} dS' \qquad \vec{k}_o \in C_+ \tag{13}$$

$$a_j(\vec{k}_o) \equiv -\frac{ik_o}{8\pi^2} \iint_{S_o} \left\{ (\hat{n}_o \times \vec{E}_o^+)\cdot(\hat{a}_j \times i\vec{k}_o) + [\hat{n}_o \times (\nabla' \times \vec{E}_o^+)]\cdot\hat{a}_j \right\} e^{-i\vec{k}_o\cdot\vec{r}'} dS' \qquad \vec{k}_o \in C_- \tag{14}$$

where $\vec{f}(\vec{k}_o) = \sum_{j=1}^{2} f_j(\vec{k}_o)\,\hat{a}_j$ and analogously for $a_j(\vec{k}_o)$.

The elimination of the surface fields will be done by another application of the integral representation Eq. (3). This time S consists of S_1 and a finite part of S_o and an upper half sphere, such that outside S is inside V_1. Let the radius of the half sphere go to infinity and assume as before the appropriate radiation conditions. We get:

$$\left.\begin{matrix}\vec{E}_1(\vec{r}) \\ \vec{0}\end{matrix}\right\} = -\nabla \times \iint_{S_o} \hat{n}_o \times \vec{E}_1^-(\vec{r}')\, G(\vec{r},\vec{r}';k_1)\, dS' -$$

$$- k_1^{-2} \nabla \times \left\{ \nabla \times \iint_{S_o} \hat{n}_o \times (\nabla' \times \vec{E}_1^-(\vec{r}'))\, G(\vec{r},\vec{r}';k_1)\, dS' \right\} +$$

$$+ \nabla \times \iint_{S_1} \hat{n}_1 \times \vec{E}_1^+(\vec{r}')\, G(\vec{r},\vec{r}';k_1)\, dS' +$$

$$+ k_1^{-2} \nabla \times \left\{ \nabla \times \iint_{S_1} \hat{n}_1 \times (\nabla' \times \vec{E}_1^+(\vec{r}'))\, G(\vec{r},\vec{r}';k_1)\, dS' \right\} \quad \begin{cases} \vec{r} \in V_1 \\ \vec{r} \notin V_1 \end{cases} \qquad (15)$$

We will primarily use the equation above when $\vec{r}$ is outside V_1. First we introduce suitable expansions of the surface fields $\hat{n}_o \times \vec{E}_1^-$ and $\hat{n}_1 \times \vec{E}_2^-$. In [4] the following expansions were introduced:

$$\hat{n}_o \times \vec{E}_1^-(\vec{r}') = \int_0^{2\pi} d\beta_1\, \hat{n}_o \times \left\{ \int_{C_-} \vec{\alpha}(\vec{k}_1) + \int_{C_+} \vec{\beta}(\vec{k}_1) \right\} e^{i\vec{k}_1 \cdot \vec{r}'} \sin\alpha_1\, d\alpha_1 \qquad (16)$$

$$\hat{n}_1 \times \vec{E}_2^-(\vec{r}') = \sum_n \alpha_n\, \hat{n}_1 \times \mathrm{Re}\, \vec{\Psi}_n(k_2 \vec{r}') \qquad (17)$$

The expansion on the surface S_o is an expansion in plane waves, both up- and downgoing while on S_1 we use an expansion in regular spherical vector waves. Furthermore, the determination of the coefficients in the related expansions of the relevant derivatives of these fields can be discussed in a way which is directly analogous to the lossless case. (However, we emphasize that considerable work remains to be done in order to determine the class of surfaces S_o and S_1 for which the required relations between the expansion coefficients is rigorously valid [1], [3], [4].) The completeness of these expansions in the lossless case is found in [4] and in the lossy case the derivation is formally analogous.

The application of the integral representation Eq. (15) inside V_2 and above S_o is formally the same as in the lossless case and for details in this matter we refer to Ref. [4]. The boundary conditions, Eq. (2), the surface field expansions, Eq. (16)-(17), and the expansion of the Green's dyadic in spherical vector waves, Eq. (9), are applied and we get:

$$\int_0^{2\pi} d\beta_1 \int_{C_+} \vec{\beta}(\vec{k}_1)\, e^{i\vec{k}_1\cdot\vec{r}} \sin\alpha_1\, d\alpha_1 = -i \sum_{nn'} \vec{\psi}_n(k_1\vec{r})\, Q_{nn'}(Re_1, Re)\, \alpha_{n'} \qquad (18)$$

$$\int_0^{2\pi} d\beta_1 \int_{C_-} \vec{\alpha}(\vec{k}_1)\, e^{i\vec{k}_1\cdot\vec{r}} \sin\alpha_1\, d\alpha_1 = i \sum_{nn'} Re\,\vec{\psi}_n(k_1\vec{r})\, Q_{nn'}(Out_1, Re)\, \alpha_{n'} \qquad (19)$$

The first equation holds for all $\vec{r}$ above S_o and outside the circumscribing sphere of S_1, while the Eq. (19) holds for all $\vec{r}$ inside the inscribed sphere of S_1. The derivation of these two equations in the lossless case relies on a "limiting absorption principle", i.e. the wave number has a small imaginary part, which eventually goes to zero. However, in the situation treated here, when losses are present no such limiting procedure is necessary. The derivation of the Eqs. (18)-(19) are otherwise analogous to the lossless case. Furthermore, we have introduced the Q'_{nn}-matrices of the scatterer S_1,

$$Q_{nn'}(Out_1, Re) \equiv k_1 \iint_{S_1} \hat{n}_1 \cdot \left\{ (\nabla' \times \vec{\psi}_n(k_1\vec{r}')) \times Re\,\vec{\psi}_{n'}(k_2\vec{r}') + c_1 \vec{\psi}_n(k_1\vec{r}') \times (\nabla' \times Re\,\vec{\psi}_{n'}(k_1\vec{r}')) \right\} dS' \qquad (20)$$

and $Q_{nn'}(Re,Re)$ is analogously defined but with regular spherical vector waves in all places.

The next step will be to eliminate the $\vec{r}$ dependence in the two equations above. In the first equation we make use of the

transformation between plane and spherical vector waves, see Eq. (6). As was pointed out above, the integral over α,β on both sides are a two-dimensional Fourier integral in k_x,k_y and by use of the inverse transform on a plane z=constant we obtain

$$\vec{\beta}(\vec{k}_1) = \frac{1}{2\pi} \sum_{nn'} \vec{B}_n(\hat{k}_1)\, Q_{nn'}(Re_1, Re)\, \alpha_{n'} \qquad \vec{k}_1 \in C_+ \tag{21}$$

In Eq. (19) we first make a scalar multiplication on both sides with $\vec{A}_n(\hat{r})$ followed by an integration over the unit sphere. We get by use of Eq. (10)

$$\int_0^{2\pi} d\beta_1 \int_{C_-} \vec{\alpha}(\vec{k}_1) \cdot \vec{B}_n^{\dagger}(\hat{k}_1) \sin\alpha_1\, d\alpha_1 = -\frac{1}{4\pi} \sum_{n'} Q_{nn'}(Out_1, Re)\, \alpha_{n'} \tag{22}$$

where $\vec{B}_n^{\dagger}(\hat{k})$ is identical to $\vec{B}_n(\hat{k})$, but with $(-i)^{\ell+2-\tau}$ exchanged with $i^{\ell+2-\tau}$.

The derivation of Eq. (21) relies on the inverse two-dimensional Fourier transform and it should here be noted the importance of expanding the transformation, see Eq. (6), and the surface field Eq. (16) in terms of integrals with the same contours $C_{\pm}$. For both this transformation and the surface fields we have the possibility of choosing different integration contours (cf. the appendix for a discussion of the more detailed choice of contours). However, when applying the inverse transform we then have to pay attention to the analytic properties of the integrands, since when the contours differ from $C_{\pm}$, k_x and k_y are not real everywhere. In this paper we will always use the $C_{\pm}$ contours, i.e. the contours where both k_x and k_y are real, and in this way we can avoid any discussion of the analytic properties.

In [4] the field $\vec{E}_o^{sc.}$ was calculated. In the case where losses are present the derivation of this field is formally identical, and will therefore only be outlined here without any details. Here we will focus on the field in V_1, which in e.g. many prospecting applications is of great importance.

The field in V_1 is given by Eq. (15). The elimination of the surface fields in this equation will be quite analogous to the computation of the field $\vec{E}_o^{sc.}$. It is also obvious that the derivation below are valid also in the lossless case. The most straightforward region to compute the field $\vec{E}_1$ in is outside the circumscribing sphere of S_1, i.e. when $r > \max_{\vec{r}' \in S_1} |r'|$. In this special case we can make use of the same expansion of the Green's dyadic over the whole surface S_1, i.e. in spherical waves. However, we note that calculations of the scattered field in V_1 inside the circumscribing sphere of S_1 can also be made, with the appropriate modifications (for "near-field" calculations within the T-matrix approach see e.g. Bringi and Seliga [9]). The surface field expansions, Eq. (16)-(17), are inserted and we get (the derivation of this equation is analogous to the Eq. (19), and again, as pointed out above, we do not rely on any "limiting absorption principle" in this lossy case):

$$\vec{E}_1(\vec{r}) = \int_0^{2\pi} d\beta_1 \int_{C_-} \vec{\alpha}(\vec{k}_1)\, e^{i\vec{k}_1\cdot\vec{r}} \sin\alpha_1 d\alpha_1 - i \sum_{nn'} \vec{\psi}_n(k_1\vec{r})\, Q_{nn'}(Re, Re)\, \alpha_{n'} \qquad (23)$$

The prescribed incoming field amplitude $\vec{a}(\vec{k}_o)$ in Eq. (14) is now used to eliminate the surface field expansion amplitudes $\vec{\alpha}(\vec{k}_1)$, $\vec{\beta}(\vec{k}_1)$ and α_n'. We insert Eq. (2) and (16) in Eq. (14) and get:

$$a_j(\vec{k}_0) = i \sum_{j'=1}^{2} \int_0^{2\pi} d\beta_1 \left\{ \int_{C_-} \alpha_{j'}(\vec{k}_1) + \int_{C_+} \beta_{j'}(\vec{k}_1) \right\} Q_{jj'}(\vec{k}_0, \vec{k}_1) \sin\alpha_1 \, d\alpha_1$$

$$\vec{k}_0 \in C_- \qquad (24)$$

Here we have introduced the generalization of the $Q_{nn'}$-matrix Eq. (20) to the infinite surface S_o:

$$Q_{jj'}(\vec{k}_0, \vec{k}_1) \equiv \frac{k_0}{8\pi^2} \iint_{S_0} \left\{ (\hat{n} \times \hat{a}_{j'}) \cdot (i\vec{k}_0 \times \hat{a}_j) - c_0 [\hat{n}_0 \times (i\vec{k}_1 \times \hat{a}_{j'})] \cdot \hat{a}_j \right\} e^{i(\vec{k}_0 - \vec{k}_1)\cdot\vec{r}'} dS' \qquad (25)$$

The formal solution of Eq. (21), (22) and (24) will be found by an elimination of the $\alpha_{n'}$-coefficients in Eq. (21) and (22)

$$\vec{\beta}(\vec{k}_1) = 2 \sum_{nn'} \vec{B}_n(\hat{k}_1) T_{nn'} c_{n'} \qquad (26)$$

where

$$c_n \equiv \int_0^{2\pi} d\beta_1 \int_{C_-} \vec{\alpha}(\vec{k}_1) \cdot \vec{B}_n^{\dagger}(\hat{k}_1) \sin\alpha_1 \, d\alpha_1 \qquad (27)$$

$$T_{nn'} \equiv - \sum_{n''} Q_{nn''}(Re, Re) \, Q^{-1}_{n''n'}(Out, Re) \qquad (28)$$

The c_n-quantity is the spherical projection of the plane wave amplitude $\vec{\alpha}(\vec{k}_1)$ later determined by a matrix equation. The T matrix characterize the scatterer S_1, i.e. it contains its shape, boundary conditions etc. If we encounter a situation where we have several buried scatterers or inhomogeneous ones the formal structure of the equation is the same, but with the relevant T-matrix inserted.

We proceed by formally inverting Eq. (24) (this can be done algebraically when S_0 is a plane, see below) and we get with Eq. (26)

$$\alpha_j(\vec{k}_1) = -i \sum_{j'} \int_0^{2\pi} d\beta_0 \int_{C_-} a_{j'}(\vec{k}_0)\, Q^{-1}_{j'j}(\vec{k}_1,\vec{k}_0)\, \sin\alpha_0\, d\alpha_0 +$$

$$+ 2 \sum_{nn'j'} \int_0^{2\pi} d\beta_1' \int_{C_+} B_{nj'}(\hat{k}_1')\, T_{nn'}\, c_{n'}\, R_{jj'}(\vec{k}_1,\vec{k}_1')\, \sin\alpha_1'\, d\alpha_1' \qquad \vec{k}_1 \in C_- \quad (29)$$

Here $B_{nj} \equiv \vec{B}_n \cdot \hat{a}_j$ and similarly $B^{\dagger}_{nj} \equiv \vec{B}^{\dagger}_n \cdot \hat{a}_j$ is defined. The reflection coefficient $R_{jj'}(\vec{k}_1,\vec{k}_1')$ for the surface S_0 from below is analogous to the T-matrix for the scatterer S_1 and is defined as:

$$R_{jj'}(\vec{k}_1,\vec{k}_1') \equiv -\sum_{j''} \int_0^{2\pi} d\beta_0 \int_{C_-} Q^{-1}_{jj''}(\vec{k}_1,\vec{k}_0)\, Q_{j''j'}(\vec{k}_0,\vec{k}_1')\, \sin\alpha_0\, d\alpha_0$$

$$\vec{k}_1' \in C_+ , \ \vec{k}_1 \in C_- \quad (30)$$

We construct the basic matrix equation for determining the coefficients c_n by multiplying Eq. (29) with $B^{\dagger}_{nj}(\hat{k}_1)$ and sum over j and integrate over β_1 and α_1 over a C_- contour. We get:

$$c_n + \sum_{n'} A_{nn'} c_{n'} = d_n \quad (31)$$

where

$$A_{nn'} \equiv -2 \sum_{n''jj'} \int_0^{2\pi} d\beta_1 \int_{C_-} \sin\alpha_1\, d\alpha_1 \int_0^{2\pi} d\beta_1' \int_{C_+} \sin\alpha_1'\, d\alpha_1' \times$$

$$\times B_{n''j'}(\hat{k}_1')\, T_{n''n'}\, R_{jj'}(\vec{k}_1,\vec{k}_1')\, B^{\dagger}_{nj}(\hat{k}_1) \quad (32)$$

$$d_n \equiv -i \sum_{jj'} \int_0^{2\pi} d\beta_1 \int_{C_-} \sin\alpha_1\, d\alpha_1 \int_0^{2\pi} d\beta_0 \int_{C_-} \sin\alpha_0\, d\alpha_0\, a_{j'}(\vec{k}_0)\, Q^{-1}_{jj'}(\vec{k}_1,\vec{k}_0)\, B^{\dagger}_{nj}(\hat{k}_1) \quad (33)$$

Thus we obtain an equation which is formally the same as in the

lossless case. Again the iteration of Eq. (31) reflect the multiple scattering phenomenon between the surface S_o and the scatterer S_1, and we refer to [4] for more details on this subject.

The final expression for the field $\vec{E}_1$ outside the circumscribing sphere of S_1, Eq. (23), can eventually be written in terms of the c_n-vector by introducing the Eqs. (29), (22), (27) and (28)

$$\vec{E}_1(\vec{r}) = \sum_{jj'} \int_0^{2\pi} d\beta_1 \int_{C_-} \hat{a}_j e^{i\vec{k}_1\cdot\vec{r}} \Big\{ -i \int_0^{2\pi} d\beta_0 \int_{C_-} a_{j'}(\vec{k}_0) Q^{-1}_{jj'}(\vec{k}_0,\vec{k}_1) \sin\alpha_0 \, d\alpha_0 +$$

$$+ 2 \sum_{nn'} \int_0^{2\pi} d\beta_1' \int_{C_+} B_{nj'}(\hat{k}_1') T_{nn'} c_{n'} R_{jj'}(\vec{k}_1,\vec{k}_1') \sin\alpha_1' \, d\alpha_1' \Big\} \sin\alpha_1 \, d\alpha_1 -$$

$$- 4\pi i \sum_{nn'} \vec{\psi}_n(k_1\vec{r}) T_{nn'} c_{n'} =$$

$$= \vec{E}_1^{\,dir.}(\vec{r}) + \sum_{nn'} \vec{\mathcal{F}}_n(\vec{r}) T_{nn'} c_{n'} - 4\pi i \sum_{nn'} \vec{\psi}_n(k_1\vec{r}) T_{nn'} c_{n'} \qquad (34)$$

The total field $\vec{E}_1$ has been divided into three terms with the following definitions:

$$\vec{E}_1^{\,dir.}(\vec{r}) \equiv -i \sum_{jj'} \int_0^{2\pi} d\beta_1 \int_{C_-} \hat{a}_j e^{i\vec{k}_1\cdot\vec{r}} \int_0^{2\pi} d\beta_0 \int_{C_-} a_{j'}(\vec{k}_0) Q^{-1}_{jj'}(\vec{k}_0,\vec{k}_1) \sin\alpha_0 \, d\alpha_0 \sin\alpha_1 \, d\alpha_1 \qquad (35)$$

$$\vec{\mathcal{F}}_n(\vec{r}) \equiv 2 \sum_{jj'} \int_0^{2\pi} d\beta_1 \int_{C_-} \hat{a}_j e^{i\vec{k}_1\cdot\vec{r}} \int_0^{2\pi} d\beta_1' \int_{C_+} B_{nj'}(\hat{k}_1') R_{jj'}(\vec{k}_1,\vec{k}_1') \sin\alpha_1' \, d\alpha_1' \sin\alpha_1 \, d\alpha_1 \qquad (36)$$

The field $\vec{E}_1^{\,dir.}$ is the transmitted field as if no scatterer is present, while the two remaining terms reflect the presence of

the scatterer; a field which could be called the scattered field $\vec{E}_1^{sc.}$. In terms of a multiple scattering interpretation, which is discussed in more detail in [4], the second term on the right hand side of Eq. (34) can be interpreted as the sum of all those contributions, which is reflected the last time at the surface S_o. Similarly, the third term corresponds to the contributions reflected the last time from the inhomogeneity. Of course both these contributions added contain all the multiple scattering effects between S_o and the inhomogeneity, via c_n, the solution of Eq. (31).

As we have seen, the consideration of the field $\vec{E}_1$ is quite analogous to the derivation of the scattered field $\vec{E}_0^{sc.}$ in V_0, which in the lossless case is found in [4]. In the lossy case the formal derivation of $\vec{E}_o^{sc.}$ is the same and we here just state the result.

$$\vec{E}_o^{sc.}(\vec{r}) = \vec{E}_o^{sc.,dir.}(\vec{r}) + \vec{E}_o^{sc.,anom.}(\vec{r}) = \vec{E}_o^{sc.,dir.}(\vec{r}) + \sum_{nn'} \vec{F}_n(\vec{r})\, T_{nn'}\, c_{n'} \tag{37}$$

where

$$\vec{E}_o^{sc.,dir.}(\vec{r}) \equiv \sum_{jj'} \int_0^{2\pi} d\beta_o \int_{C_+} \hat{a}_j\, e^{i\vec{k}_o\cdot\vec{r}} \int_0^{2\pi} d\beta_o' \int_{C_-} R_{jj'}(\vec{k}_o,\vec{k}_o')\, a_{j'}(\vec{k}_o') \sin\alpha_o' d\alpha_o' \sin\alpha_o d\alpha_o$$

$$\vec{F}_n(\vec{r}) \equiv -2i \sum_{jj'} \int_0^{2\pi} d\beta_o \int_{C_+} \hat{a}_j\, e^{i\vec{k}_o\cdot\vec{r}} \int_0^{2\pi} d\beta_1 \int_{C_+} B_{nj'}(\hat{k}_1) \Big[Q_{jj'}(\vec{k}_o,\vec{k}_1) +$$

$$+ \sum_{j''} \int_0^{2\pi} d\beta_1' \int_{C_-} Q_{jj''}(\vec{k}_o,\vec{k}_1')\, R_{j''j'}(\vec{k}_1',\vec{k}_1) \sin\alpha_1' d\alpha_1' \Big] \sin\alpha_1 d\alpha_1 \sin\alpha_o d\alpha_o \tag{38}$$

$$R_{jj'}(\vec{k}_o,\vec{k}_o') \equiv -\sum_{j''} \int_0^{2\pi} d\beta_1 \int_{C_-} Q_{jj''}(\vec{k}_o,\vec{k}_1)\, Q^{-1}_{j''j'}(\vec{k}_1,\vec{k}_o') \sin\alpha_1 d\alpha_1 \quad \vec{k}_o \in C_+,\ \vec{k}_o' \in C_- \tag{39}$$

$R_{jj'}(\vec{k}_o, \vec{k}_o')$ is the reflection coefficient for the surface S_o from above, cf. Eq. (30).

So far we have considered the general case, and have not introduced any specific geometry. The inversion of Eq. (24) in the general case, when S_o is rough, is indeed a difficult problem. However, when one has a "finite hill" one can find an algorithm so that the interaction between the hill and the inhomogeneity is taken into account [10]. The numerical computations in this paper will only consider a plane surface S_o and for this case most of the equations can be simplified. We get for a plane surface S_o ($z=z_o$=constant) (cf. the lossless case):

$$\vec{E}_1^{dir.}(\vec{r}) = \sum_j \frac{2}{k_o} \int_0^{2\pi} d\beta_1 \int_{C_-} \hat{a}_j e^{i\vec{k}_1\cdot\vec{r}} a_j(\vec{k}_1^{*-}) e^{iz_o((k_1^2-\lambda_1^2)^{1/2}-(k_o^2-\lambda_1^2)^{1/2})} \frac{k_1(k_1^2-\lambda_1^2)^{1/2}}{\Delta_j(\lambda_1)} \sin\alpha_1 d\alpha_1 \quad (40)$$

$$\vec{F}_n(\vec{r}) = -2\sum_j \int_0^{2\pi} d\beta_1 \int_{C_-} \hat{a}_j e^{i\vec{k}_1\cdot\vec{r}} B_{nj}(\hat{k}_1^-) R_j(\lambda_1) e^{2iz_o(k_1^2-\lambda_1^2)^{1/2}} \sin\alpha_1 d\alpha_1 \quad (41)$$

$$A_{nn'} = 2\sum_{n''j} \int_0^{2\pi} d\beta_1 \int_{C_-} B_{nj}^{\dagger}(\hat{k}_1) B_{n''j}(\hat{k}_1^-) R_j(\lambda_1) e^{2iz_o(k_1^2-\lambda_1^2)^{1/2}} \sin\alpha_1 d\alpha_1 \, T_{n''n'} \quad (42)$$

$$d_n = \sum_j \int_0^{2\pi} d\beta_o \int_{C_-} a_j(\vec{k}_o) B_{nj}^{\dagger}(\hat{k}_o^{*-}) e^{iz_o((k_1^2-\lambda_o^2)^{1/2}-(k_o^2-\lambda_o^2)^{1/2})} \frac{2(k_o^2-\lambda_o^2)^{1/2}}{\Delta_j(\lambda_o)} \sin\alpha_o d\alpha_o \quad (43)$$

$$\vec{E}_o^{sc.,dir.}(\vec{r}) = \sum_j \int_0^{2\pi} d\beta_o \int_{C_+} a_j(\vec{k}_o^-) R_j(\lambda_o) e^{-2iz_o(k_o^2-\lambda_o^2)^{1/2}+i\vec{k}_o\cdot\vec{r}} \hat{a}_j \sin\alpha_o d\alpha_o \quad (44)$$

$$\vec{F}_n(\vec{r}) = \frac{4c_o k_o}{k_1} \sum_j \int_0^{2\pi} d\beta_o \int_{C_+} e^{i\vec{k}_o\cdot\vec{r}+iz_o((k_1^2-\lambda_o^2)^{1/2}-(k_o^2-\lambda_o^2)^{1/2})} B_{nj}(\hat{k}_o^{*+}) \hat{a}_j \frac{(k_o^2-\lambda_o^2)^{1/2}}{\Delta_j(\lambda_o)} \sin\alpha_o d\alpha_o \quad (45)$$

The Fresnel reflection coefficients are [11] :

$$R_1(\lambda) \equiv \frac{N_1(\lambda)}{D_1(\lambda)} \equiv \frac{c_0 k_1 \left(1-(\lambda/k_0)^2\right)^{1/2} - k_0 \left(1-(\lambda/k_1)^2\right)^{1/2}}{c_0 k_1 \left(1-(\lambda/k_0)^2\right)^{1/2} + k_0 \left(1-(\lambda/k_1)^2\right)^{1/2}} \tag{46}$$

$$R_2(\lambda) \equiv \frac{N_2(\lambda)}{D_2(\lambda)} \equiv \frac{\left(k_0^2-\lambda^2\right)^{1/2} - c_0 \left(k_1^2-\lambda^2\right)^{1/2}}{\left(k_0^2-\lambda^2\right)^{1/2} + c_0 \left(k_1^2-\lambda^2\right)^{1/2}}$$

R_1 is the reflection coefficient for an incoming wave polarized along $\hat{a}_1$ and R_2 for a wave polarized along $\hat{a}_2$. $D_j(\lambda)$ and $N_j(\lambda)$ are the denominator and nominator in the reflection coefficient respectively, and $\lambda_i = k_i \sin\alpha_i$; $i=0,1$. All square roots are defined such that $\mathrm{Im}(k_i^2-\lambda_i^2)^{1/2} \geq 0$. We have also introduced the follwoing notation for the transformed arguments in Eq. (40)-(45)

$$\vec{k}_1^{\,x-} \equiv k_1 \left(\sin\alpha_1 \cos\beta_1, \sin\alpha_1 \sin\beta_1, -\left(\left(\frac{k_0}{k_1}\right)^2 - \sin^2\alpha_1\right)^{1/2}\right)$$

$$\hat{k}_1^{-} \equiv \left(\sin\alpha_1 \cos\beta_1, \sin\alpha_1 \sin\beta_1, -\cos\alpha_1\right)$$

$$\vec{k}_0^{-} \equiv k_0 \left(\sin\alpha_0 \cos\beta_0, \sin\alpha_0 \sin\beta_0, -\cos\alpha_0\right)$$

$$\hat{k}_0^{x\pm} \equiv \frac{k_0}{k_1} \left(\sin\alpha_0 \cos\beta_0, \sin\alpha_0 \sin\beta_0, \pm\left(\left(\frac{k_0}{k_1}\right)^2 - \sin^2\alpha_0\right)^{1/2}\right)$$

III. Numerical applications

The final Eqs. (40)-(45) given in the preceding section will now be applied in some numerical examples. These illustrations include both field computations above the ground (the electric field) and below the interface (the magnetic field). The source that excites the inhomogeneity is chosen to be a vertical dipole source; in the case of electric field an electric dipole, while in the magnetic case a magnetic dipole. The dipole source located at a source point $P\equiv(\rho_t,0,z_t)$ is given by [11]:

$$\left.\begin{matrix}\vec{E}_o^{inc.}(\vec{r})\\ \vec{H}_o^{inc.}(\vec{r})\end{matrix}\right\} = \frac{1}{k_o^2}\nabla\times\left\{\nabla\times\left[\hat{z}\,\frac{e^{ik_o|\vec{r}-\vec{r}_t|}}{k_o|\vec{r}-\vec{r}_t|}\right]\right\} \tag{47}$$

If we place the source on the surface S_o ($z_t=z_o$) then Eq. (43) simplifies into

$$d_n = \frac{2k_1\gamma_n}{ik_o\sqrt{\ell(\ell+1)}}\int_{i\infty}^{1}\frac{i^{m-\ell}\,k_o t\,dt}{k_o\left(1-\left(\frac{k_o}{k_1}\right)^2(1-t^2)\right)^{1/2}+c_o k_1 t}\; e^{ik_1 z_o\left(1-\left(\frac{k_o}{k_1}\right)^2(1-t^2)\right)^{1/2}}\times$$

$$\times\, J_m(k_o s_t(1-t^2)^{1/2})\left\{im\,\delta_{\sigma o}\delta_{\tau 1}\,P_\ell^m\left(\left(1-\left(\frac{k_o}{k_1}\right)^2(1-t^2)\right)^{1/2}\right)-\right.$$

$$\left.-\delta_{\sigma e}\delta_{\tau 2}\left[(\ell-m+1)\,P_{\ell+1}^m\left(\left(1-\left(\frac{k_o}{k_1}\right)^2(1-t^2)\right)^{1/2}\right)-(\ell+1)\left(1-\left(\frac{k_o}{k_1}\right)^2(1-t^2)\right)^{1/2}P_\ell^m\left(\left(1-\left(\frac{k_o}{k_1}\right)^2(1-t^2)\right)^{1/2}\right)\right\} \tag{48}$$

Here the definitions of spherical harmonics and normalization follow Ref. [4].

The numerical examples are separated into two groups; one in which we compute the electric field above the ground and one

where we focus on the magnetic field below the interface. In all numerical examples we have chosen a moderate contrast in the parameters between V_o and V_1. These values are chosen here since they are believed to illustrate "worst case" applications of the above formalism (i.e. using the full structure of the equations, without further specializations). Numerical computations for values of the parameters corresponding to high contrasts and losses will be performed in the future. In this case it is possible to introduce further simplications by using asymptotic methods for the strongly oscillating integrals. Work in this direction is in progress. Parameters in common in all the numerical examples are:

$$k_1^2/k_0^2 = 10 + 5i$$

$$\mu_{1r}/\mu_{0r} = 1$$

$$k_0 z_0 = 0.8$$

The inhomogeneity, completely specified by its T-matrix, is here taken as a perfectly conducting spheroid. The semiaxis in the direction of rotational symmetry is a and the semiaxis in the perpendicular direction is b. The T-matrix for the spheroid is generated numerically for an orientation of the rotational symmetry axis along the z-axis, and is then rotated by means of the three-dimensional rotation matrices [12] to an arbitrary orientation. The orientation of the symmetry axis is given in spherical angles ϕ, χ. This procedure allows us to calculate the T-matrix for inhomogeneities which are asymmetrically oriented both with respect to the interface and to the source position. The generation of the

T-matrix for a large class of asymmetrical scatterers can thus be performed efficiently, since the rotational matrices are fairly easy to generate numerically. To get the result for a different orientation of the scatterer only these matrices have to be recalculated; the T-matrix along the symmetry axis is the same as before. The steps of computation of the scattered field for a given inhomogeneity are in short:

1) Compute the d_n-vector, Eq. (48) for a given source position P.

2) Compute the $A_{nn'}$-matrix, Eq. (42).

3) Compute the field vector $\vec{F}_n(\vec{r})$ or $\vec{\mathcal{F}}_n(\vec{r})$, Eq. (41) or (45) for a given array of field points $\vec{r}$.

4) Generate the $T_{nn'}$-matrix of the inhomogeneity oriented along the z-axis.

5) Rotate the $T_{nn'}$-matrix by applying the rotation matrices.

6) Solve Eq. (31) for the c_n-vector.

7) Combine the quantities in Eq. (37) or (34).

A variation of a single parameter or a different choice of inhomogeneity (concerning e.g. both shape and orientation) does not affect all steps above; most of them need not be repeated. Only a few items have to be recalculated and this feature makes the formalism efficient in situations where one is interested exploring the effect of these types of parameter variations.

Many of the quantities contain an integral over a C_+ or C_- contour. These integrals have to be computed numerically, and we use a fast, improved quadrature, which in a subdivision of the integration interval uses the previously computed function va-

lues. The integrand usually contains an exponential factor, which makes the convergence very rapid. In those integrals where such an exponential factor is absent or is small, we use a different method. Since the integrals have oscillating integrands we divide the integration interval into parts, according to e.g. the nulls of the integrand so that the total integral becomes an alternating series. We then apply an Euler transformation to the series, which improves the convergence of the series very efficiently.

The computer time required in the various steps above varies considerably and only a rough estimate can be given. The steps 1), 2), 4), 5), 7) have usually an execution time of less than 2 min. c.p.u. on an IBM 370/3031 or IBM 360/65. Item 3) is the most time-consuming step, which for an array size $\vec{r}$ and a truncation order used in the numerical examples considered here, takes about 10 min. c.p.u. The radial and the azimuthal dependence in the pertinent integrals can be separated in such a way that all azimuthal dependence is a common factor outside a remaining integral, which only depends on the ρ and z coordinates. Step 6) takes only a couple of seconds c.p.u. to evaluate. However, it should be noted that the various execution times here given highly depend on the truncation size of the matrices, prerequired accuracy in the evaluation of the integrals, array size of measuring points in $\vec{F}_n(\vec{r})$ or $\vec{\mathcal{F}}_n(\vec{r})$ etc., and we should also observe that the constituent parts in the scheme above can be used again in various combinations which reduces the computational costs considerably. The above c.p.u. times refer to computations to about three significant figures in the final results. In many practical applications one

does not of course need such a high accuracy and the c.p.u. time requirements are reduced accordingly.

In a series of plots, Figures 3-6, we illustrate the anomalous scattered electric field on the surface S_o ($z=z_o$) in a region close to the inhomogeneity. These plots show computer interpolated surfaces of constant amplitude of the anomalous scattered electric field $E_o^{sc.,anom.}$. Due to the computer interpolation algorithm these figures contain some irregularities, which are not present in the original computations. These figures show different field components for various scatterers, which are perfectly conducting spheroids - both prolate and oblate - of diverse orientations, both with respect to the surface S_o and to the source position. In Fig. 7 we show the quotient of the vertical components of the anomalous scattered electric field and the incoming electric field along the x-axis. The pattern these plots exhibit are fairly complex, but seem to fit reasonably well to the radiation pattern of a simple dipole, which replaces the scatterer. In order to achieve this the orientation of the dipole has to be adjusted. The resulting optimal orientation was found to agree reasonably well with what was to be expected from the relevant source, treated as a source in a homogeneous space (no interface S_o). The present more accurate computations can be used to investigate when these simple dipole-excitation models are valid.

The second part of the numerical illustrations given in this paper is the magnetic field below the surface S_o. Here we have calculated the magnetic field - both the direct and scattered - along a straight line with a specific direction. Along these "drillholes" the field component along the line is depicted in

Fig. 8-10. The "drillhole" starts at the coordinates (x_o, y_o, z_o) and has a direction given by the spherical angles (η, ψ). The source in these calculations is a vertical magnetic dipole located on the surface S_o at $(\rho_t, 0, z_o)$. In each plot we illustrate the field component along the drillhole for various scatterers - perfectly conducting spheroid of different orientations. As expected we get the highest response from the obstacle at the position closest to the inhomogeneity. Although the scatterer is rather small and the drillhole does not come too near the obstacle, we have a rather high signal return from the inhomogeneity, which in some situations is more than 10%.

Acknowledgements

The author wishes to thank Dr. Staffan Ström for reading the entire manuscript carefully. The present work is sponsored by the National Swedish Board for Technical Development (STU) and their support is gratefully acknowledged.

Appendix

Transformation relations between plane and spherical vector waves.

The transformation between spherical waves and plane waves for a real wave number is discussed in detail in [13]. The extension to complex wave numbers is found in this appendix.

Consider the following integral for $z>0$:

$$\int_0^{2\pi} d\beta \int_{C_+} Y_n(\hat{k})\, e^{i\vec{k}\cdot\vec{r}} \sin\alpha\, d\alpha \tag{A.1}$$

Here we have adopted the notations

$$\begin{aligned}
&\vec{r} \equiv (x,y,z) \equiv r\hat{r} \\
&\hat{r} \equiv (\sin\theta\cos\phi,\ \sin\theta\sin\phi,\ \cos\theta) \\
&\vec{k} \equiv (k_x,k_y,k_z) \equiv k\hat{k} \equiv |k|e^{i\mathcal{H}}\hat{k} \\
&\hat{k} \equiv (\sin\alpha\cos\beta,\ \sin\alpha\sin\beta,\ \cos\alpha)
\end{aligned} \tag{A.2}$$

The complex contour C_+ in the α-plane (see Figure 2) is a contour from $\alpha=0$ to $\alpha=\pi/2-\mathcal{H}-i\infty$ subject to ($\alpha=\alpha'+i\alpha''$, where α',α'' are real numbers).

$$\tanh\alpha'' + \tan\alpha' \tan\mathcal{H} = 0 \tag{A.3}$$

We will here assume $\mathcal{H}\in(0,\pi/4)$. This restriction can be relaxed but it is sufficiently general for our purpose (remember $\mathrm{Im}k^2\geq 0$, $\mathrm{Re}k^2>0$). The case $\mathcal{H}=0$ is excluded since that is the situation analysed by Danos and Maximon [13].

The integral in Eq. (A.1) is essentially a two-dimensional Fouriertransform in (k_x,k_y); first rewritten in polar coordinates $\lambda=k\sin\alpha$ and β and then finally transformed into the spherical angles α,β. For more details see Banos [14]. We have here explicitly assumed $z>0$ ($\phi<\pi/2$) but for $z<0$ the C_+-contour is replaced by the C_--contour and a similar analysis will hold. Note that on both these contours we have

$$\begin{aligned} &\mathrm{Im}(k\sin\alpha)=0 \\ &\mathrm{Im}(zk\cos\alpha)\gtrless 0 \\ &\mathrm{Re}(k\sin\alpha)\gtrless 0 \end{aligned} \qquad (A.4)$$

The C_+-contour defined by Eq. (A.3) transformed to the $t=\cos\alpha$-plane is a contour (see Figure 11) from $t=\infty e^{i(\pi/2-\varkappa)}$ to $t=1$ subject to ($t=t'+it''$)

$$(t'\tan\varkappa+t'')(t'-t''\tan\varkappa)=\tan\varkappa \qquad (A.5)$$

The integral (A.1) is easily shown to be uniformly convergent for all $\vec{r}$ when $z\gtrless c>0$, where c is any positive number (cf. the exponential decaying factor). We also note that the integrand is an analytic function except for the branch points $t=\pm1$ of the associated Legendre functions $P_\ell^m(\cos\alpha)$ in $Y_n(\hat{k})$ and for the essential singularity at infinity for the exponential function. It is permitted to deform the contour C_+ to any contour Γ provided no singularities are crossed. For convenience we will deform the C_+-contour to Γ as depicted in Figure 12 or in the $\cos\alpha$-plane, see Fig. 13. The constant $\alpha_o=\pi/2-i\alpha_o''$ is any complex number where α_o''

satisfies

$$\sinh \alpha_0'' \geq 1/\cos\theta \qquad \text{(A.6)}$$

The reason for this deformation of C_+ is to simplify the analysis given below. We note that the first part of Γ (from $\alpha=0$ to $\alpha=\alpha_0$) is identical to the corresponding part of the contour used in [13].

The evaluation of the integral in Eq. (A.1) is done by first making a rotation of the coordinate system (α,β) to a coordinate system (η,ψ). Here η is the new polar angle, specified as the angle between $\vec{k}$ and $\vec{r}$, and ψ is the new azimuthal angle (see Fig. 14). The spherical harmonics $Y_n(\hat{k})$ is transformed according to [12]:

$$Y_n(\alpha,\beta) = \sum_{m'} \mathcal{D}^{(\ell)}_{m'm}(\phi,\theta,0)\, Y_{\ell m'}(\eta,\psi) \qquad \text{(A.7)}$$

This relation holds for real angles (α,β), but can be analytically continued to complex angles (α,β) (note that the m' summation is finite). We have here changed from real combinations of the spherical harmonics to complex ones which have an azimuthal dependence $e^{im\beta}$ (this is merely a matter of convenience and in accordance with references [12] and [13]). The final result holds for real combinations too. Furthermore, we can without loss of generality take $\phi=0$. The case $\phi\neq 0$ is an azimuthal rotation with a trivial shift in the β interval. The relation between the two coordinate systems (α,β) and (η,ψ) is [12] $(\phi=0)$:

$$\begin{aligned}
\cos\eta &= \sin\theta\sin\alpha\cos\beta + \cos\theta\cos\alpha \\
\sin\eta\cos\psi &= \cos\theta\sin\alpha\cos\beta - \sin\theta\cos\alpha \\
\sin\eta\sin\psi &= \sin\alpha\sin\beta
\end{aligned} \qquad \text{(A.8)}$$

The Eq. (A.1) can be rewritten as

$$\int_0^{2\pi} d\beta \int_\Gamma Y_n(\hat{k})\, e^{i\vec{k}\cdot\vec{r}} \sin\alpha\, d\alpha =$$

$$= \sum_{m'} \mathcal{D}^{(\ell)}_{m'm}(0,\theta,0) \int_{\gamma'} d\psi \int_{\Gamma'} Y_{\ell m'}(\eta,\psi)\, e^{ikr\cos\eta} \left|\frac{\partial(\alpha,\beta)}{\partial(\eta,\psi)}\right| \sin\alpha\, d\eta \qquad (A.9)$$

The Jacobian $\left|\frac{\partial(\alpha,\beta)}{\partial(\eta,\psi)}\right|$ is easily found:

$$\left|\frac{\partial(\alpha,\beta)}{\partial(\eta,\psi)}\right| \sin\alpha = \left[\frac{\partial\alpha}{\partial\eta}\frac{\partial\beta}{\partial\psi} - \frac{\partial\alpha}{\partial\psi}\frac{\partial\beta}{\partial\eta}\right] \sin\alpha = \sin\eta$$

We observe that the Jacobian is non-zero for $|\cos\eta| \neq 1$, and thus the transformation non-singular, see [13] and below.

$$\int_0^{2\pi} d\beta \int_\Gamma Y_n(\hat{k})\, e^{i\vec{k}\cdot\vec{r}} \sin\alpha\, d\alpha =$$

$$= \sum_{m'} \mathcal{D}^{(\ell)}_{m'm}(0,\theta,0) \int_{\gamma'} d\psi \int_{\Gamma'} Y_{\ell m'}(\eta,\psi)\, e^{ikr\cos\eta} \sin\eta\, d\eta \qquad (A.10)$$

The contours γ' and Γ' are the transformed contours of the (α,β) variables given by Eq. (A.8). (Note that Γ' is a function of ψ.)

Our goal is now to deform the contours in the right hand side of Eq. (A.10) to the original contours ($\psi\in[0,2\pi]$ and $\eta\in\Gamma$ or equivalently $\eta\in C_+$). For this step to be valid we have to make sure that no singularities of the integrand are crossed. The endpoints of the integral also have to be the same.

In the discussion of the contour deformations it is convenient to divide Γ into two parts: one from the origin to the point α_o and from α_o to infinity respectively. The deformation of the first part of the Γ contour, where α is real and $\alpha=\pi/2+i\alpha''$, $-\alpha''_o \leq \alpha'' \leq 0$

is found in [13]. There a detailed analysis is found of how to rearrange the integrations in the real region, and how to let the starting point of the η variable remain at $\eta=0$ ($\alpha\to 0$ corresponds to $\eta\to\theta$). We see that the map of the real part of Γ is real, and the rearrangement can be interpreted as a transformation on the unit sphere. A discussion of how to circumvent the singular points $\cos\eta=\pm 1$ is also found in [13]. The rearrangement discussed above can also be performed for the original contour C_+, but then much harder to illustrate.

We now discuss the final part of the Γ' contour, i.e. $\alpha=\alpha'-i\alpha''_o$, $\arctan\left(\frac{\tanh\alpha''_o}{\tan\varkappa}\right)\lesssim\alpha'\lesssim\pi/2$ and $\alpha\in C_+$, $\alpha''\lesssim-\alpha''_o$. First we analyse the asymptotic behaviour of Γ' as $\alpha\to\pi/2-\varkappa-i\infty$. According to Eq. (A.8) we have:

$$\cos\eta=\sin\theta\sin\alpha\cos\beta+\cos\theta\cos\alpha$$

Asymptotically we have

$$\arg(\cos\eta)=-\varkappa+\pi/2-\arctan(\tan\theta\cos\beta)\qquad \alpha''\to-\infty \qquad (A.11)$$

and we see that $\arg(\cos\eta)\in[\pi/2-\varkappa-\theta,\ \pi/2-\varkappa+\theta]$, see Fig. 15. Furthermore we have

$$\arg(k\cos\eta)=\pi/2-\arctan(\tan\theta\cos\beta)\qquad \alpha''\to-\infty \qquad (A.12)$$

and we conclude that $\arg(k\cos\eta)\in[\pi/2-\theta,\ \pi/2+\theta]$ as $\alpha''\to-\infty$. Thus for $\theta<\pi/2$ we have $\arg(k\cos\eta)\in(0,\pi)$ as $\alpha''\to-\infty$, which ensures the correct convergence properties at infinity. In the η-plane this corresponds to (see Figure 16)

$$\eta \to -\varkappa + \pi/2 - \arctan(\tan\theta\cos\beta) - i\infty \qquad \alpha \to \pi/2 - \varkappa - i\infty$$

The remaining step is to make sure that we do not cross the singular points $\cos\eta = \pm 1$ as we deform the remaining part of Γ'. We have, see Eq. (A.8)

$$\cos\eta = \sin\alpha \sin\theta \cos\beta + \cos\alpha \cos\theta$$

It is fairly easy to see that for $\alpha = \alpha' + i\alpha''$ with α' arbitray and $\alpha'' \lesseqgtr -\alpha_0''$, where α_0'' is given by Eq. (A.6) we have

$$|\cos\eta| > 1$$

Thus we see that the last part of Γ' ($\alpha = \alpha' + i\alpha''$, $\alpha'' \lesseqgtr -\alpha_0''$) does not enclose the singular points $\cos\eta = \pm 1$. Neither does the last part of Γ' enclose both $\cos\eta = 1$ and $\cos\eta = -1$, since the curve never enters the third quadrant of the $\cos\eta$ plane. (The last part of Γ' starts in the first or second quadrant, depending on β, and ends in the sector $\arg(\cos\eta) \in [\pi/2 - \varkappa - \theta,\ \pi/2 - \varkappa + \theta]$, and the first part of Γ', where α is real or $\alpha = \pi/2 + i\alpha''$; $-\alpha_0'' \lesseqgtr \alpha'' \lesseqgtr 0$, has only values in the first and second quadrant).

The integration variable ψ can then easily be changed to the real interval $\psi \in [0, 2\pi]$. The endpoints of the deformed curve remain the same; we have $\psi = n\pi$ when $\beta = n\pi$. From Eq. (A.8) we can solve for ψ, and we get ($\psi = \psi' + i\psi''$ and see Fig. 17):

$$\begin{cases} \tan 2\psi' = \dfrac{2A\sin\beta}{A^2 + B^2 - \sin^2\beta} \\ \tanh 2\psi'' = \dfrac{2B\sin\beta}{A^2 + B^2 + \sin^2\beta} \end{cases} \qquad \text{(A.13)}$$

where

$$\begin{cases} A \equiv \cos\theta\cos\beta - \sin\theta\tan\alpha'(1-\tanh^2\alpha'')(\tanh^2\alpha'' + \tan^2\alpha')^{-1} \\ B = -\sin\theta\tanh\alpha''(1+\tan^2\alpha')(\tanh^2\alpha'' + \tan^2\alpha')^{-1} \end{cases}$$

Thus we have analysed the contours γ' and Γ' and justified the deformation of these contours to the original $\psi\in[0,2\pi]$ and $\eta\in\Gamma$ or $\eta\in C_+$ and showed that this deformation is valid. We have, see Eq. (A.10)

$$\int_0^{2\pi} d\beta \int_{C_+} Y_n(\hat{k})\, e^{i\vec{k}\cdot\vec{r}} \sin\alpha\, d\alpha = \sum_{m'} \mathcal{D}^{(\ell)}_{m'm}(\phi,\theta,0) \int_0^{2\pi} d\psi \int_{C_+} Y_{\ell m'}(\eta,\psi)\, e^{ikr\cos\eta} \sin\eta\, d\eta$$

$$= \mathcal{D}^{(\ell)}_{0m}(\phi,\theta,0)\, 2\pi\gamma_{\ell 0} \int_{C_+} P_\ell(\cos\eta)\, e^{ikr\cos\eta} \sin\eta\, d\eta =$$

$$= 2\pi i^\ell h^{(1)}_\ell(kr)\, Y_n(\hat{r}) \equiv 2\pi i^\ell \psi_n(k\vec{r}) \qquad \text{(A.14)}$$

In this last equation we have returned to the more general situation where $\phi\neq 0$, see the discussion above, and furthermore we have used the integral representation of $h^{(1)}_\ell(z)$ [15] and the definitions of $\mathcal{D}^{(\ell)}_{m'm}(\phi,\theta,0)$ [12], i.e.

$$h^{(1)}_\ell(z) = i^{-\ell} \int_{\infty\exp(i\nu)}^{1} P_\ell(t)\, e^{izt}\, dt \qquad \nu\in(-\arg z, \pi-\arg z)$$

$$\mathcal{D}^{(\ell)}_{0m}(\phi,\theta,0) = Y_n(\hat{r})/\gamma_{\ell 0} \qquad \gamma_{\ell 0} = \sqrt{\frac{2\ell+1}{4\pi}}$$

A completely analogous analysis can be made for $z<0$ but this time with the contour C_- and we can here conclude:

$$\psi_n(k\vec{r}) = \frac{1}{2\pi i^\ell} \int_0^{2\pi} d\beta \int_{C_\pm} Y_n(\hat{k})\, e^{i\vec{k}\cdot\vec{r}} \sin\alpha\, d\alpha \qquad z\gtrless 0 \qquad \text{(A.15)}$$

For an $z \neq 0$ the integral in Eq. (a.15) is a uniformly convergent integral and differentiation under the integral sign can be justified. The spherical vector waves $\vec{\psi}_n(k\vec{r})$ can thus be formed

$$\vec{\psi}_{\tau n}(k\vec{r}) \equiv \frac{1}{\sqrt{\ell(\ell+1)}} \left(\frac{1}{k} \nabla \times\right)^{\tau} \left(k\vec{r}\, \psi_n(k\vec{r})\right) \qquad \tau = 1,2 \qquad \text{(A.16)}$$

In proving the transformation between spherical vector waves and plane vector waves we will essentially follow the presentation found in [8]. First we consider:

$$\vec{\psi}_{1n}(k\vec{r}) = h_\ell^{(1)}(kr)\, \vec{A}_{1n}(\hat{r}) \qquad \text{(A.17)}$$

For definition of the vector spherical harmonics see [4]. We will also need the following identity [6]. (Note that we for convenience are using the complex combination of the spherical harmonics, i.e. no σ index.)

$$\begin{aligned} \vec{A}_{1n}(\hat{r}) = \vec{A}_{1m\ell}(\hat{r}) &= \frac{1}{\sqrt{\ell(\ell+1)}} \nabla Y_{\ell m}(\hat{r}) \times \hat{r} = \\ &= a_- Y_{\ell m+1}(\hat{r})\, \hat{\varepsilon}_- + a_+ Y_{\ell m-1}(\hat{r})\, \hat{\varepsilon}_+ + a_z Y_{\ell m}(\hat{r})\, \hat{z} \end{aligned} \qquad \text{(A.18)}$$

where a_-, a_+, a_z are contants depending only on ℓ and m and where

$$\begin{cases} \hat{\varepsilon}_+ = \frac{1}{\sqrt{2}} (\hat{x} + i\hat{y}) \\ \hat{\varepsilon}_- = \frac{1}{\sqrt{2}} (\hat{x} - i\hat{y}) \end{cases} \qquad \text{(A.19)}$$

We get with Eq. (A.15)

$$\vec{\psi}_{1n}(k\vec{r}) = h_\ell^{(1)}(kr)\left[a_- Y_{\ell m+1}(\hat{r})\hat{\varepsilon}_- + a_+ Y_{\ell m-1}(\hat{r})\hat{\varepsilon}_+ + a_z Y_{\ell m}(\hat{r})\hat{z}\right] =$$

$$= \frac{1}{2\pi i^\ell}\int_0^{2\pi} d\beta \int_{C_\pm} \vec{A}_{1n}(\hat{k})\, e^{i\vec{k}\cdot\vec{r}} \sin\alpha\, d\alpha \qquad z \gtrless 0 \tag{A.20}$$

The spherical vector wave for $\tau=2$ is found by differentiation under the integral sign, and we get

$$\vec{\psi}_{2n}(k\vec{r}) = \frac{1}{k}\nabla \times \vec{\psi}_{1n}(k\vec{r}) =$$

$$= \frac{i}{2\pi i^\ell}\int_0^{2\pi} d\beta \int_{C_\pm} \vec{A}_{2n}(\hat{k})\, e^{i\vec{k}\cdot\vec{r}} \sin\alpha\, d\alpha \qquad z \gtrless 0 \tag{A.21}$$

Thus finally we have

$$\vec{\psi}_n(k\vec{r}) = \frac{i}{2\pi}\int_0^{2\pi} d\beta \int_{C_\pm} \vec{B}_n(\hat{k})\, e^{i\vec{k}\cdot\vec{r}} \sin\alpha\, d\alpha \qquad z \gtrless 0 \tag{A.22}$$

where $\vec{B}_n(\hat{k})$ is defined in Eq. (7).

References

1. P.C. Waterman, J. Acoust. Soc. Am. 45, 1417-1429 (1969); Phys. Rev. D3, 825-839 (1971); J. Acoust. Soc. Am. 60, 567-580 (1976).

2. V. Varatharajulu and Y-H. Pao, J. Acoust. Soc. Am. 60, 556-566 (1976).

3. G. Kristensson and S. Ström, J. Acoust. Soc. Am. 64, 917-936 (1978).

4. G. Kristensson, "Electromagnetic Scattering from Buried Inhomogeneities - a General Threedimensional Formalism", Report 78-42, Inst. of Theor. Physics, Göteborg (1978).

5. A. Boström and G. Kristensson, "Elastic wave scattering by a three-dimensional inhomogeneity in an elastic half-space", Report 79-33, Inst. of Theor. Physics, Göteborg (1979).

6. P.M. Morse and H. Feshbach, Methods of Theoretical Physics (McGraw-Hill, N.Y. 1953).

7. Handbook of Mathematical Functions, edited by M. Abramowitz and I.A. Stegun (National Bureau of Standards, Applied Math. Series No 55, 1970).

8. A.J. Devaney and E. Wolf, J. Math. Phys. 15, 234-244 (1974).

9. V.N. Bringi and T.A. Seliga, "Surface currents and near zone fields using the T-matrix", Recent developments in Classical wave scattering: Focus on the T-matrix approach, International symposium and workshop, Ohio State University, Columbus, Ohio, June 25-27 (1979).

10. G. Kristensson and S. Ström, Scattering from inhomogeneities below a non-planar interface, Report TMF 79-1, Inst. of Theor. Physics, Göteborg (1979).

11. J.A. Stratton, Electromagnetic Theory (McGraw-Hill, N.Y. 1941).

12. A.R. Edmonds, Angular Momentum in Quantum Mechanics (Princeton University, Princeton, N.J. 1974).

13. M. Danos and L.C. Maximon, J. Math. Phys. 6, 766-778 (1965).

14. A. Baños, Dipole Radiation in the Presence of a Conducting Half-Space (Pergamon, N.Y. 1966).

15. G.N. Watson, A Treatise on the Theory of Bessel Functions (Cambridge University Press, Cambridge 1966).

Figure captions

Fig. 1 Geometry and notations.

Fig. 2 The integration contours C_+ and C_-, $\varkappa = \arg k$

Fig. 3 The amplitude of the x-component of the anomalous scattered field $|\vec{E}_o^{sc.,anom.} \cdot \hat{x}|$ on the surface S_o ($k_o z_o = 0.8$) for a buried perfectly conducting spheroid. The semi axis in the direction of rotational symmetry is $k_o a = 0.3$ and the other semi axis is $k_o b = 0.15$. The orientation of the symmetry axis is $\theta = \chi = \pi/6$. The source is located at $k_o \rho_t = 6$ and the scale factor is 10^{-6}.

Fig. 4 The same as Fig. 3 but the z-component $|\vec{E}_o^{sc.,anom.} \cdot \hat{z}|$ shown and $\theta = \pi/3$, $\chi = \pi/2$, $k_o \rho_t = 3$ and the scale factor is 10^{-5}.

Fig. 5 The same as Fig. 3 but $k_o a = 0.15$, $k_o b = 0.3$ and $\theta = \pi/6$, $\chi = 3\pi/4$, $k_o \rho_t = 3$ and the scale factor is 10^{-5}.

Fig. 6 The same as Fig. 3 but $k_o a = 0.15$, $k_o b = 0.3$, $k_o \rho_t = 0$ and the scalar factor is 10^{-4}.

Fig. 7 The variation in $|\vec{E}_o^{sc.,anom.} \cdot \hat{z}| / |\vec{E}_o^{inc.} \cdot \hat{z}|$ for data as in Fig. 5 along the x-axis. The scale is in percent.

Fig. 8 The amplitude and phase variation of the field component of the scattered magnetic field $\hat{n} \cdot \vec{H}_1^{sc.}$ along a drillhole (t is a parameter along the drillhole). The drillhole starts at $k_o(x_o, y_o, z_o) = (1, 0, 0.8)$ and has the direction $\eta = 5\pi/6$, $\psi = \pi$. The source is located at $k_o \rho_t = 3$. Data for the obstacle $k_o a = 0.1$, $k_o b = 0.2$

a) $\theta = \pi/2$, $\chi = 0$

b) $\theta = \pi/6$, $\chi = \pi/4$

Fig. 9 The amplitude of the field component of the scattered mangetic field $|\hat{n}\cdot\vec{H}_1^{sc}\cdot|$ along the drillhole $k_o(x_o,y_o,z_o)=(-1,1,0.8)$, $\eta=5\pi/6$, $\psi=3\pi/2$, $k_o\rho_t=3$ $k_oa=0.1$, $k_ob=0.2$ and a) $\theta=\pi/6$, $\chi=\pi/4$, b) $\theta=\pi/3$, $\chi=\pi/2$.

Fig. 10 The amplitude and phase variation of the field component of the total magnetic field $\hat{n}\cdot\vec{H}_1$ along the drillhole for data as in Fig. 8 b). The dashed line is field component for a homogeneous ground.

Fig. 11 The C_+ contour in the complex $\cos\alpha$-plane ($\aleph=\pi/6$).

Fig. 12 The Γ contour ($\aleph=\pi/6$).

Fig. 13 The Γ contour in the complex $\cos\alpha$-plane

Fig. 14 Notations of angles in the rotated coordinate system.

Fig. 15 The variation in $\cos\eta$ as a function of α for fixed θ (α varies along the complex part of Γ ; the dotted line is the variation of α along $\alpha=\pi/2-i\nu$, $\nu=[0,\alpha_0'']$; $\theta=5\pi/12$, $\aleph=\pi/6$ a) $\cos\beta=-1$, b) $\cos\beta=-1/2$, c) $\cos\beta=0$, d) $\cos\beta=1/2$, e) $\cos\beta=1$.

Fig. 16 The variation of η as a function of α for fixed θ. For data see Fig. 16.

Fig. 17 The variation of ψ as a function of β for fixed α ($\theta=5\pi/12$, $\aleph=\pi/6$, $\sinh\alpha''=-1/\cos\theta$, $\tan\alpha'=-\tanh\alpha''/\tan\aleph$).

Figure 1

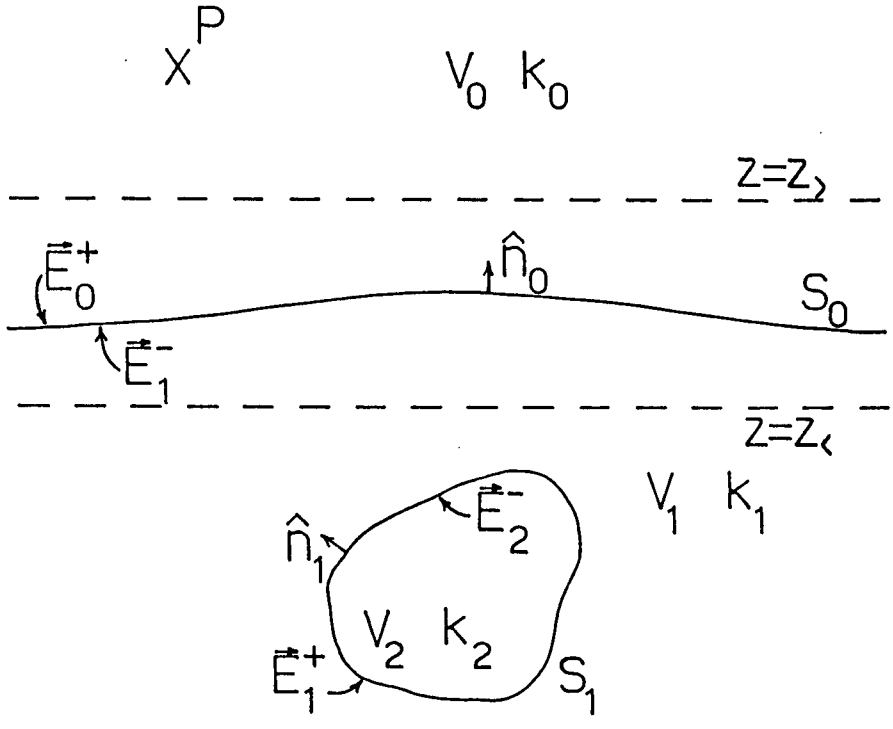
P
V_0 k_0
$z=z_>$
$\vec{E}_0^+$
$\hat{n}_0$
S_0
$\vec{E}_1^-$
$z=z_<$
V_1 k_1
$\vec{E}_2^-$
$\hat{n}_1$
V_2 k_2
$\vec{E}_1^+$
S_1

Figure 2

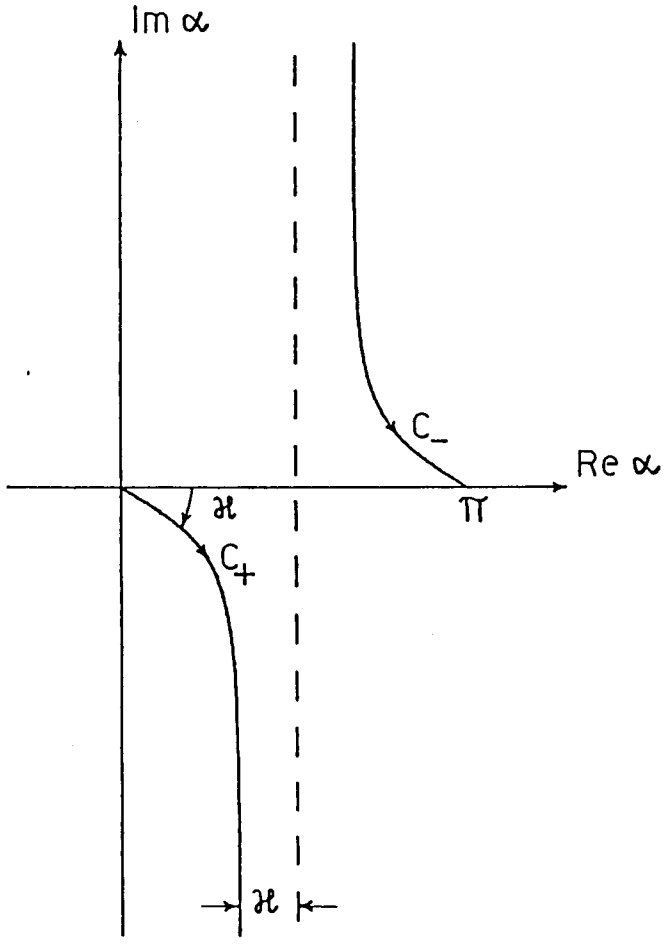

Figure 3

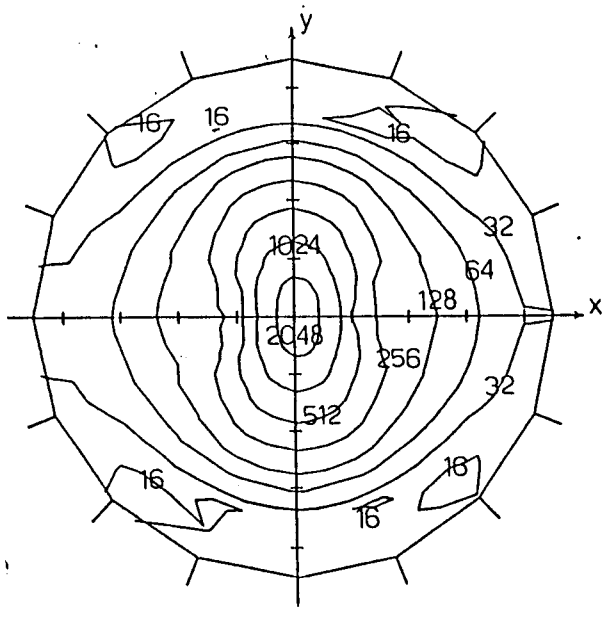

Figure 4

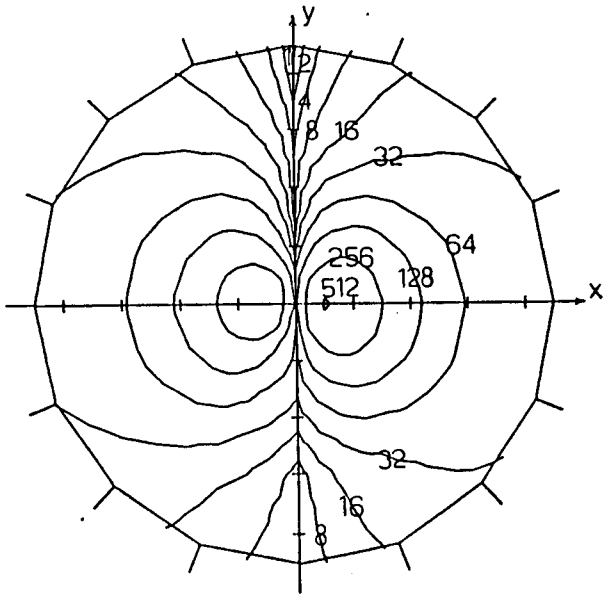

Figure 5

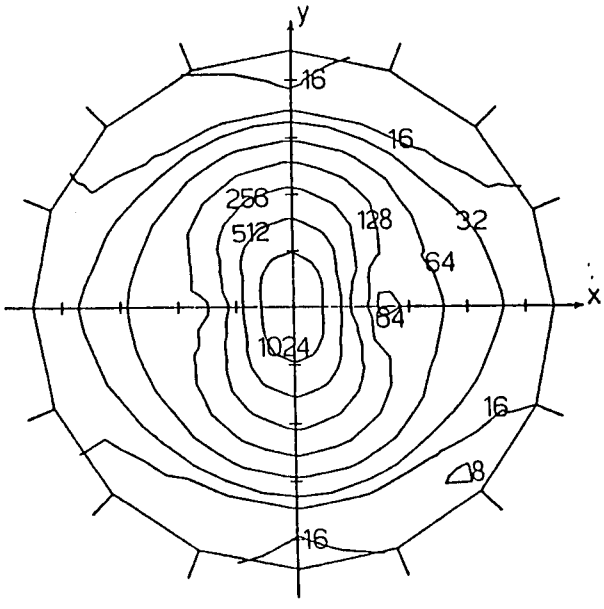

Figure 6

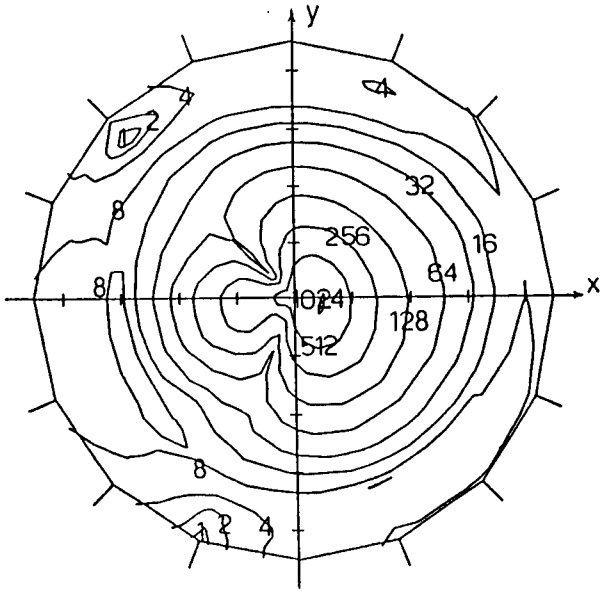

Figure 7

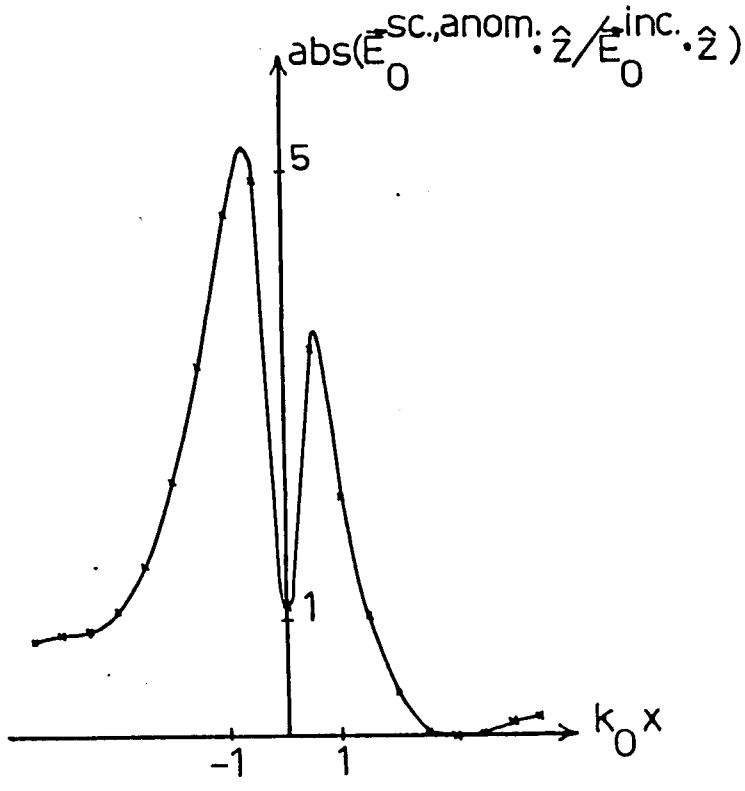

Figure 8

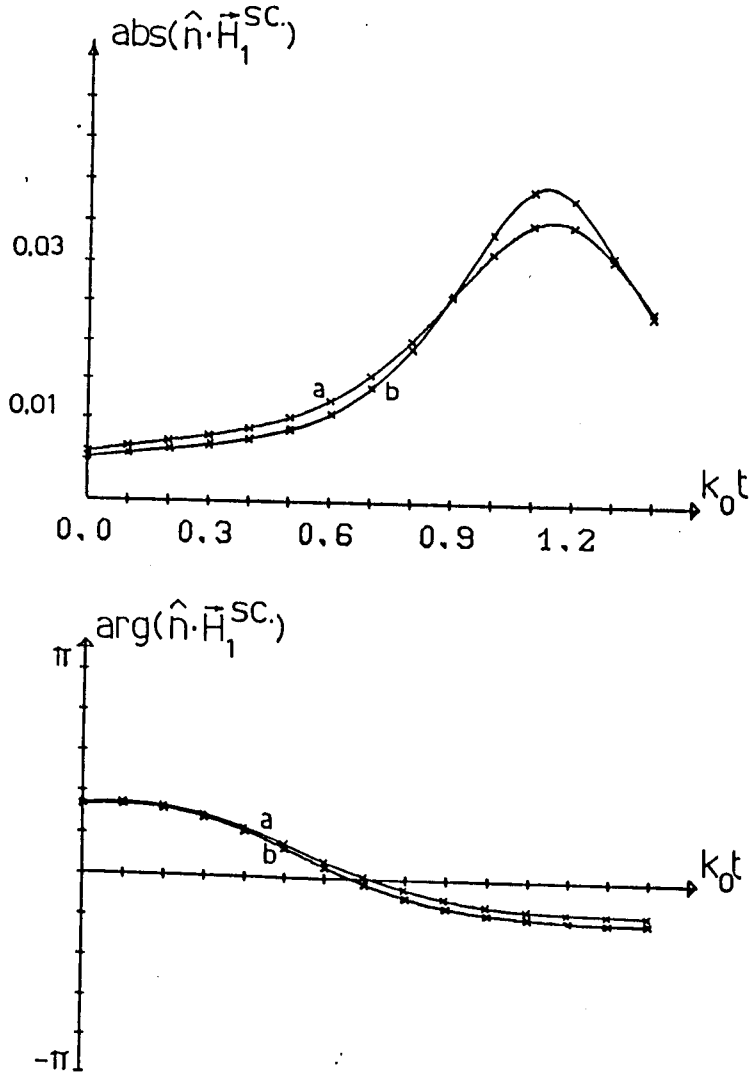
abs($\hat{n}\cdot\vec{H}_1^{sc.}$)
0.03
0.01
a
b
k_0t
0.0
0.3
0.6
0.9
1.2
arg($\hat{n}\cdot\vec{H}_1^{sc.}$)
π
-π
a
b
k_0t

Figure 9

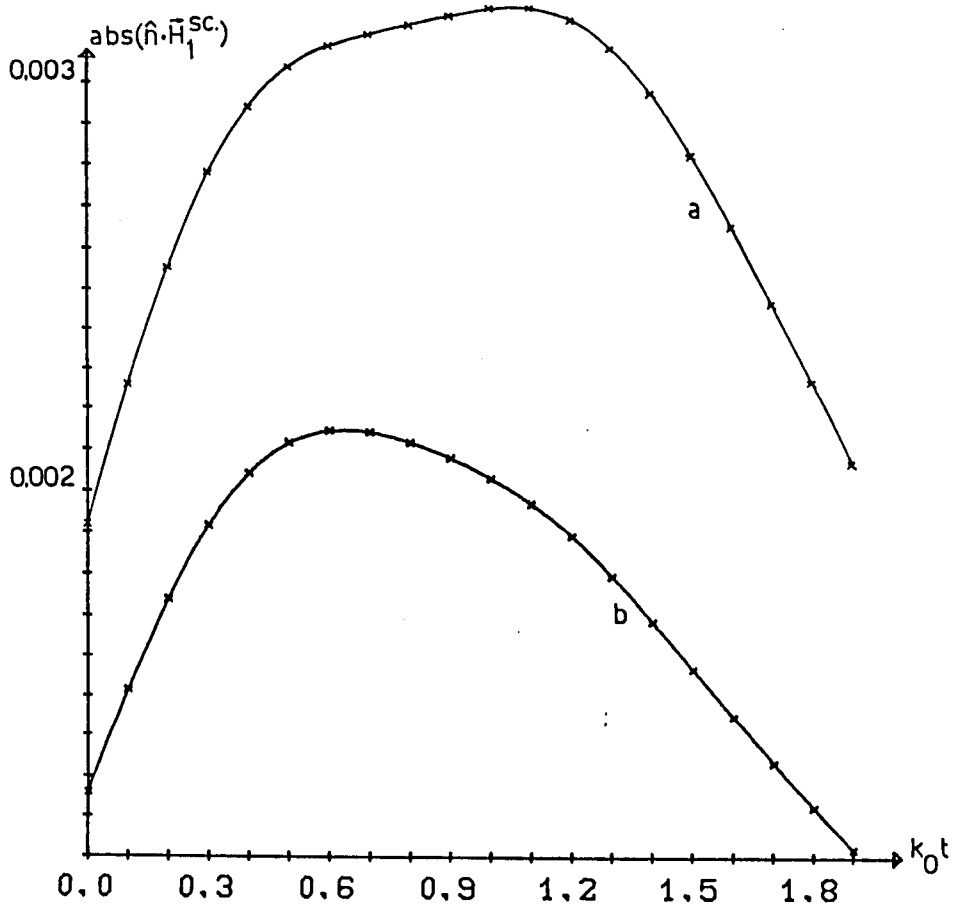

Figure 10

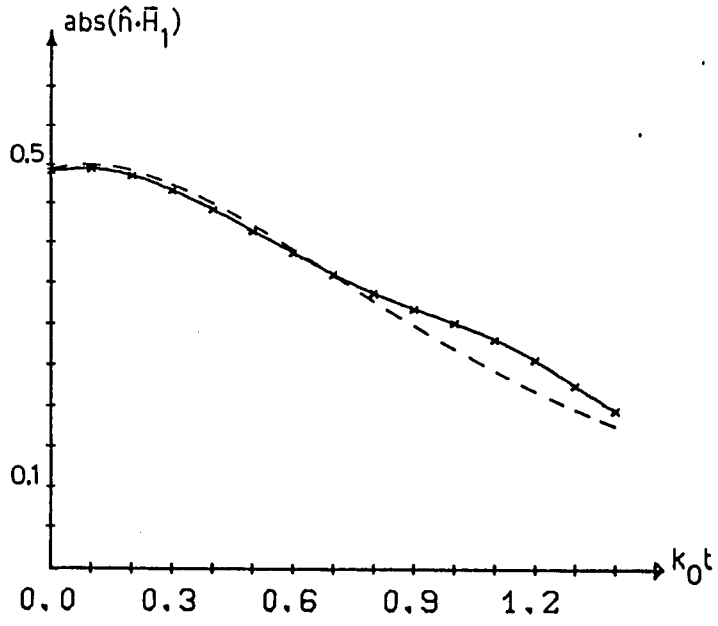

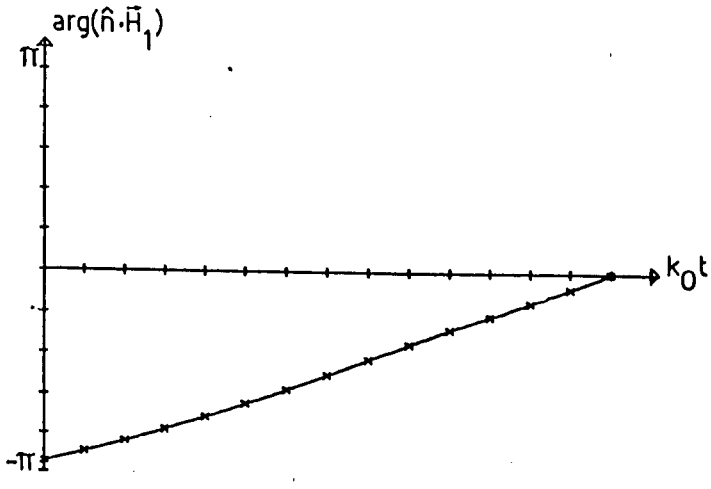

Figure 11

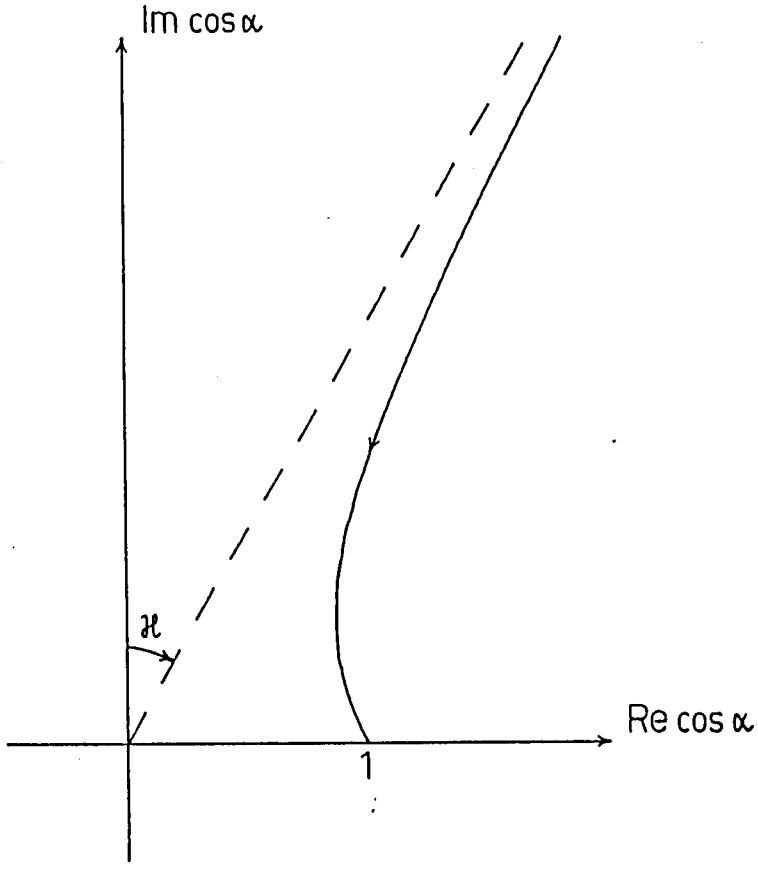

Figure 12

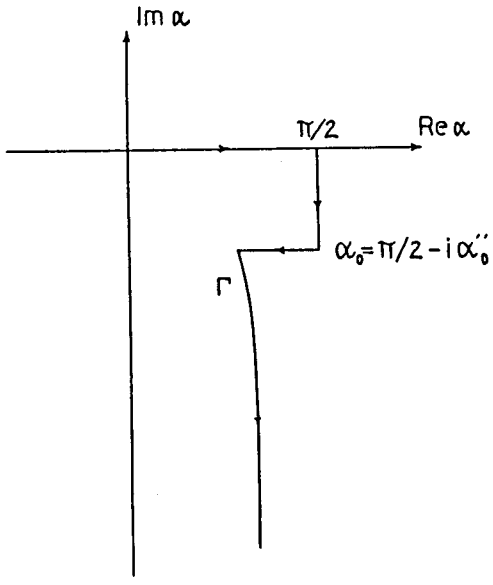

Figure 13

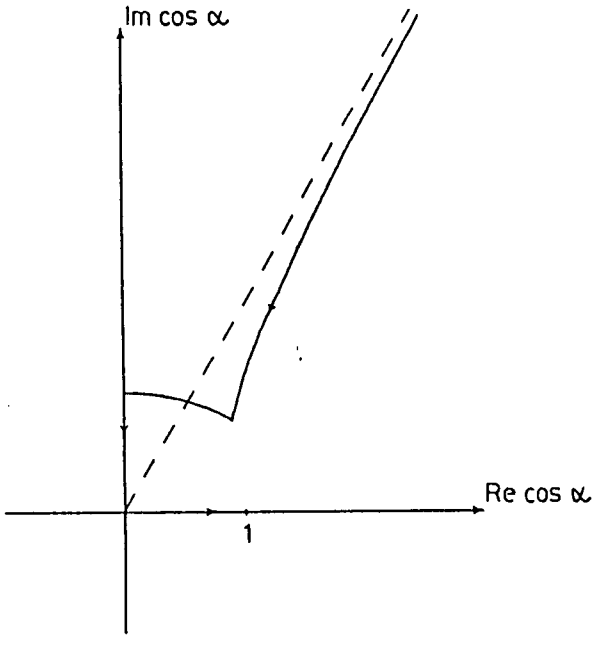

Figure 14

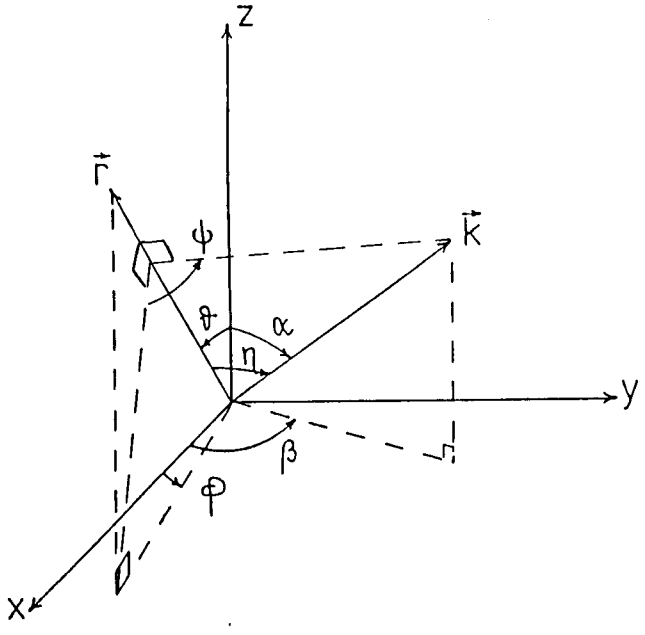

Figure 15

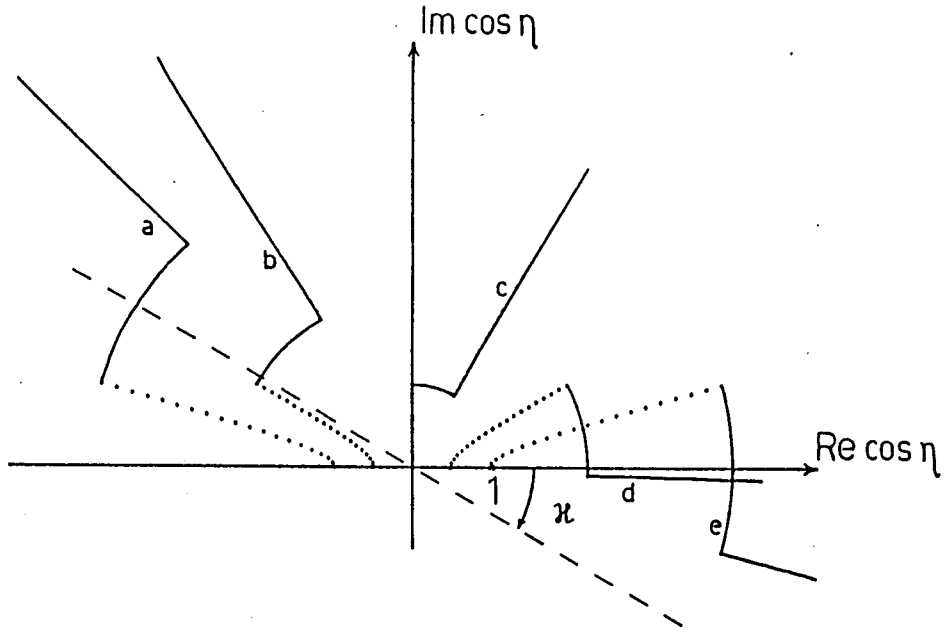

Figure 16

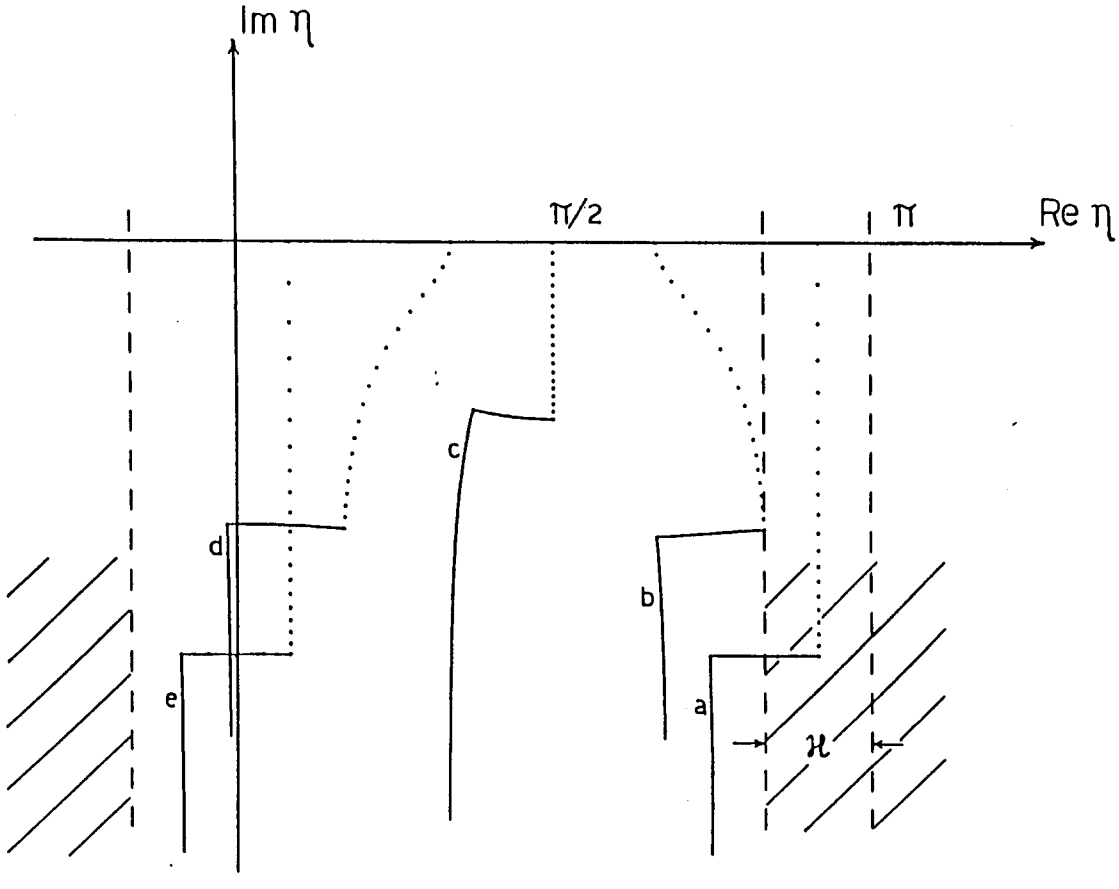

Figure 17